

# FAK Promotes Osteoblast Progenitor Cell Proliferation and Differentiation by Enhancing Wnt Signaling

Chunhui Sun,<sup>1,2</sup> Hebao Yuan,<sup>1</sup> Li Wang,<sup>1</sup> Xiaoxi Wei,<sup>1,3</sup> Linford Williams,<sup>1</sup> Paul H Krebsbach,<sup>1</sup> Jun-Lin Guan,<sup>4</sup> and Fei Liu<sup>1</sup>

<sup>1</sup>Department of Biologic and Materials Sciences and Division of Prosthodontics, University of Michigan School of Dentistry, Ann Arbor, MI, USA

<sup>2</sup>Key Laboratory for Biotechnology on Medicinal Plants of Jiangsu Province, School of Life Science, Jiangsu Normal University, Xuzhou, Jiangsu, China

<sup>3</sup>Department of Orthodontics, Jilin University School and Hospital of Stomatology, Changchun, Jilin, China

<sup>4</sup>Department of Cancer Biology, University of Cincinnati College of Medicine, Cincinnati, OH, USA

## ABSTRACT

Decreased bone formation is often associated with increased bone marrow adiposity. The molecular mechanisms that are accountable for the negative correlation between bone mass and bone marrow adiposity are incompletely understood. Focal adhesion kinase (FAK) has critical functions in proliferation and differentiation of many cell types; however, its roles in osteoblast lineage cells are largely unknown. We show herein that mice lacking FAK in Osterix-expressing cells exhibited decreased osteoblast number and low bone mass as well as increased bone marrow adiposity. The decreased bone mass in FAK-deficient mice was accounted for by decreased proliferation, compromised osteogenic differentiation, and increased adipogenic differentiation of bone marrow Osterix-expressing cells resulting from downregulation of Wnt/ $\beta$ -catenin signaling due to the reduced expression of canonical Wnt ligands. In contrast, FAK loss in calvarial preosteoblasts had no adverse effect on their proliferation and osteogenic differentiation and these cells had intact Wnt/ $\beta$ -catenin signaling. © 2016 American Society for Bone and Mineral Research.

**KEY WORDS:** OSTEOBLASTS; OSTEOPROGENITOR; FAK; WNT;  $\beta$ -CATENIN; BONE MARROW; ADIPOCYTE

## Introduction

In patients who suffer from osteoporosis<sup>(1)</sup> or conditions that can induce bone loss such as disuse,<sup>(2)</sup> microgravity exposure,<sup>(3)</sup> and estrogen insufficiency,<sup>(4)</sup> bone marrow adiposity is often significantly increased. The insight into the molecular mechanisms underlying increased bone marrow adiposity can facilitate the development of therapy of these pathological conditions.

Bone marrow mesenchymal stromal/stem cells (BMSCs) can give rise to both osteoblasts, which are responsible for the bone formation, and adipocytes, which are responsible for the marrow fat formation.<sup>(5)</sup> Thus, the negative correlation between bone mass and marrow adiposity observed in osteopenic conditions suggests that the lineage progression of BMSCs into osteoblasts and adipocytes may be coordinated. One pathway implicated in the regulation of BMSC fate and the decision to differentiate to osteoblasts or adipocyte is the canonical Wnt signaling pathway.<sup>(6)</sup>

Wnt/ $\beta$ -catenin signaling plays important roles in both osteoblastogenesis and adipogenesis.<sup>(6,7)</sup> Upon the binding of Wnt ligands to its Frizzled family receptors,  $\beta$ -catenin is stabilized and

translocated from the cytoplasm to the nucleus to stimulate the transcription of Wnt target genes.<sup>(7)</sup> Via this mechanism, Wnt/ $\beta$ -catenin signaling promotes the progression of Osterix-expressing cells to bone-producing osteoblasts.<sup>(8)</sup> Besides its indispensable role in osteoblastogenesis, Wnt/ $\beta$ -catenin signaling is a potent suppressor of adipogenesis.<sup>(6)</sup> Importantly, two recent studies demonstrated important dual roles of Wnt/ $\beta$ -catenin signaling in bone mass and bone marrow adiposity regulation. Removal of  $\beta$ -catenin in Osterix-expressing cells leads to decreased bone mass and increased bone marrow adiposity.<sup>(9,10)</sup>

FAK is an intracellular non-receptor tyrosine kinase and a major mediator of signal transduction by integrins. Since its discovery in the early 1990s, numerous studies have shown a role for FAK in the regulation of cell spreading, adhesion, migration, survival, proliferation, and differentiation.<sup>(11,12)</sup> The role of FAK in skeletal development is largely unclear. It has been shown that FAK deletion in mature osteoblasts does not affect mouse bone development, although it compromises bone healing.<sup>(13)</sup> Because FAK signaling is hyperactive in many types of cancers, many pharmaceutical inhibitors of FAK have been developed in recent years.<sup>(14)</sup> Unfortunately, it is unknown to what extent FAK inhibition would impact bone health. We

Received in original form February 16, 2016; revised form June 30, 2016; accepted July 5, 2016. Accepted manuscript online July 08, 2016.

Address correspondence to: Fei Liu, DDS, PhD, 1011 N University Ave, Department of Biologic and Materials Sciences and Division of Prosthodontics, University of Michigan, School of Dentistry, Ann Arbor, MI 48109, USA. E-mail: feiliu@umich.edu

Additional Supporting Information may be found in the online version of this article.

Journal of Bone and Mineral Research, Vol. 31, No. 12, December 2016, pp 2227–2238

DOI: 10.1002/jbmr.2908

© 2016 American Society for Bone and Mineral Research

previously demonstrated that the inhibition of FAK kinase activity by a chemical inhibitor leads to compromised mouse bone marrow osteoblast differentiation.<sup>(15)</sup> This prompted us to determine to what extent FAK may regulate the function of early osteoblast lineage cells. To this end, we generated a FAK conditional knockout mouse model in which FAK was deleted in Osterix-expressing cells. We show that this targeted deletion leads to a decrease in bone mass associated with increased bone marrow adiposity and decreased Wnt/ $\beta$ -catenin mediated transcription.

## Materials and Methods

### Mice

The floxed FAK (FAK<sup>flox/flox</sup>) mice were generated by us previously.<sup>(16)</sup> Osx-Cre transgenic mice were described previously<sup>(8)</sup> and obtained from Jackson laboratory (Bar Harbor, ME, USA). All mice were backcrossed for at least eight generations onto a C57BL/6 background. Mice were housed under pathogen-free conditions at 22  $\pm$  2°C on a 12:12-hour light/dark cycle, fed with 5001 or 5008 (for mating units) rodent diet (LabDiet, St. Louis, MO, USA). Each mating unit has one male and two female mice. Male mice were euthanized by carbon dioxide overdose at 2 months of age for bone phenotyping studies, at 6 to 8 weeks old for bone marrow cultures. Neonatal mice were euthanized by decapitation in primary calvarial osteoblast digestion experiments. All experimental procedures were carried out with the approval of the Institutional Animal Care and Use Committee at the University of Michigan.

### Immunohistochemistry

Immunohistochemistry on paraffin sections was performed as described.<sup>(17)</sup> In brief, endogenous peroxidase was blocked by 0.3% H<sub>2</sub>O<sub>2</sub>/methanol for 30 min. Sections were then incubated with FAK primary antibody C20 (Santa Cruz Biotechnology, Santa Cruz, CA, USA; sc-558) overnight at 4°C. A horseradish peroxidase–streptavidin system (DAKO, Carpinteria, CA, USA) was used to detect immunoreactivity, which was followed by counterstaining with hematoxylin.

### RNA extraction and qRT-PCR

Total RNA was isolated using Trizol reagent (Invitrogen, Carlsbad, CA, USA) according to the manufacturer's instructions. qRT-PCR analyses were performed as described.<sup>(15)</sup> cDNA templates were subjected to qPCR using the SYBR Green PCR Core reagents system (Qiagen, Valencia, CA, USA). 18S rRNA was used as an internal control. Relative gene expression was calculated by the  $\Delta$ Ct (the difference between the threshold cycles) method.<sup>(18)</sup> Primer sequences used for real-time PCR are available upon request.

### Micro-computed tomography analysis

Femora were dissected and analyzed by micro-computed tomography ( $\mu$ CT) using an eXplore Locus SP (GE Healthcare Pre-Clinical Imaging, London, ON, Canada) as described.<sup>(15)</sup> Whole calvaria were dissected and analyzed as reported<sup>(19)</sup> with modifications. In brief, fixed threshold of 1800 Hounsfield Units was used to discriminate mineralized tissue. Regions of interest (ROIs) for parietal and frontal bones were established as 0.5 mm in length, 0.5 mm in width, depth equivalent to thickness of bone, and position starting at a 1 mm distance from sagittal suture for both parietal and frontal bones, 1 mm distance from coronal suture for parietal bone, and 1.5 mm for frontal bone,

using the Advanced ROI tool. The genotype information of bone samples was blinded to the image analyzer.

### Histomorphometry

Static histomorphometry were performed similar to that described.<sup>(15,20)</sup> All parameters were measured according to the Report of the American Society of Bone and Mineral Research Histomorphometry Nomenclature Committee.<sup>(21)</sup> The genotype information of bone samples was blinded to image analyzer.

### BMSCs culture

BMSCs were obtained from bone marrow of 6-week-old to 8-week-old control or conditional knockout (CKO) mice. In brief, mice were euthanized and the femur and tibia were removed, cleaned of all connective tissue. The ends of each tibia and femur were cut and cells in bone marrow were flushed by  $\alpha$ -MEM medium with 26G syringe. After centrifugation for 5 min at 1000g, cell pellets were resuspended in medium with 18G syringe followed by filtration through a 70- $\mu$ m nylon mesh filter. Then 100 million cells were cultured in a 100-mm dish with 10 mL basic medium including  $\alpha$ -MEM medium, 10% fetal bovine serum (FBS), 100 U/mL penicillin, and 100 mg/mL of streptomycin. Nonadherent cells were removed after 3 days by discarding 5 mL medium and adding 5 mL of fresh basic medium. Every other day, cells were washed, and fresh medium was added for a period of 10 days. After confluence, cells were trypsinized by 0.25% trypsin/EDTA and  $2 \times 10^6$  cells (passage 1) were plated in a 100-mm dish. The same conditions were used for the subsequent passages.

### BMSC osteogenic differentiation and histochemical assay

BMSCs with the second passage were seeded in a 12-well plate at  $1 \times 10^5$  per well. Twenty-four hours later (designated as day 0), the basic medium were removed and replaced by induction medium, which was basic medium containing 50 mg/mL of ascorbic acid and 10 mM of beta-glycerophosphate. The induction medium was changed every 2 days for 21 days. Alkaline phosphatase staining (ALP) was performed for osteoblast differentiation at day 7 using a commercial kit (Sigma Diagnostics, Livonia, MI, USA) according to the manufacturer's instructions. Alizarin red staining (AR) was performed for mineralization analysis at day 21. In brief, cells were fixed with 70% ice-cold ethanol for 1 hour, and stained with 40 mM alizarin red S, pH 4.2, for 10 min at room temperature with rotation.

### BMSC adipocyte differentiation

BMSCs were seeded in a 12-well plate at  $4 \times 10^5$  per well. On the second day (day 0), cells were incubated with adipogenic induction medium (basic medium containing 1  $\mu$ M dexamethasone, 5  $\mu$ g/mL troglitazone, 50  $\mu$ M 3-isobutyl-1-methylxanthine, and 1  $\mu$ g/mL insulin) for 2 days and adipogenic maintenance medium (basic medium containing 1  $\mu$ g/mL insulin) for 3 days. Oil-red O staining was used to assess adipogenic differentiation at day 5. Briefly, cells were fixed with 10% formalin for 1 hour, and washed with 60% isopropanol to dehydrate. Then cells were stained with 0.2% Oil red O for 10 min at room temperature. After three washes with water, cells were visualized on light microscopy and photographed. To extract incorporated Oil red O, 1 mL 100% isopropanol was added to each well followed by 10-min gentle shaking at room temperature. The optical density (OD) values were collected at 500 nm.

## Primary calvarial osteoblast culture

Calvarial cells were isolated from 1-day-old to 3-day-old transgenic mice. After removal of sutures, parietal bones were subjected to four sequential digestions as described.<sup>(15)</sup> Cells were plated at a density of  $1.9 \times 10^4$  to  $2.4 \times 10^4$  cells/cm<sup>2</sup> in a 12-well plate in  $\alpha$ -MEM containing 10% FBS. For osteogenic differentiation, the medium was changed to differentiation medium after 1 week of culture as described.<sup>(15)</sup> ALP and AR staining were performed at day 7 and day 21, respectively.

## Proliferation assay

BMSCs from control and CKO mice were seeded in a 12-well plate at  $1 \times 10^5$ /well in differentiation medium. Cells were trypsinized 3 or 7 days later and cell numbers were counted.

## Ki67 staining

Cells were fixed in 4% paraformaldehyde (wt/vol) for 20 min at room temperature and blocked in sheep serum. Then cells were incubated with primary antibody (Ki67; Cell Signaling Technology, Beverly, MA, USA) overnight at 4°C, washed three times with PBST, and then incubated with appropriate secondary antibody for 1 hour at room temperature. After three washes, cells were mounted with ProLong Gold Anti-fade Reagent with DAPI (Life technology, Eugene, OR, USA). Ki67-positive cells were quantified by Image J software (<https://imagej.nih.gov/ij/>).

## Western blot

Cells were lysed in NP40 lysis buffer (PH 8.0 Tris-HCl 20 mM, NaCl 137 mM, 1% NP40, 10% glycerol, Na<sub>3</sub>VO<sub>4</sub> 1 mM) and boiled for 10 min. Protein extracts were analyzed by 8% (FAK,  $\beta$ -catenin, Vinculin) and 15% (p-GSK-3 $\beta$ , GSK-3 $\beta$ ) SDS-PAGE and transferred onto polyvinylidene fluoride (PVDF) membrane (Millipore, Billerica, MA, USA; IPVH00010). Membranes were incubated with rabbit anti-FAK antibody (Santa Cruz Biotechnology), mouse anti- $\beta$ -catenin antibody (BD Biosciences, San Jose, CA, USA), rabbit anti-p-GSK-3 $\beta$  antibody, rabbit anti-GSK-3 $\beta$  antibody, or mouse anti-vinculin antibody (Sigma-Aldrich, St. Louis, MO, USA) at 4°C overnight. After washing in Tris-buffered saline Tween-20 (TBST), the membrane was incubated with horseradish peroxidase-conjugated secondary antibody: Goat anti-rabbit (Thermo Fisher Scientific, Rockford, IL, USA; 31460) or Goat anti-mouse antibody (Jackson ImmunoResearch, West Grove, PA, USA; 115-035-072) for 1 hour at room temperature. Membranes were developed with HPR substrate ECL (Millipore; WBKL S0500). Films were scanned using an Epson Perfection V700 photo system (Epson, Indonesia) and bands were quantified with the optical density function of Image J software.

## Statistics

Student's *t* test was used to make comparison between the two groups. Differences were considered significant at  $p < 0.05$ .

## Results

### Deletion of FAK in Osterix<sup>+</sup> cells leads to osteopenia in mice

To assess the physiological function of FAK in early osteoblast lineage cells, we generated FAK CKO mice with *Osx*-Cre transgenic mice, which express Cre recombinase in osteoprogenitor cells.<sup>(6)</sup> Briefly, we mated floxed FAK (FAK<sup>F/F</sup>) mice (designated as control

[CTR] mice) with *Osx*-Cre transgenic mice to generate FAK<sup>F/+</sup>; *Osx*-Cre mice (designated as CHet mice), which were mated with FAK<sup>fllox/fllox</sup> mice to generate CTR mice, CHet mice, and FAK<sup>fllox/fllox</sup>; *Osx*-Cre (CKO) mice. Littermate mice were used in all experiments. The body weight of CKO mice was less than that of both CTR and CHet mice (Supporting Fig. S1). To determine the deletion of FAK in CKO bones, immunostaining was performed in both femur and calvaria. FAK was efficiently deleted in most osteoblasts and osteocytes of CKO bones (Supporting Fig. S2). Next, we used  $\mu$ CT to evaluate the effects of FAK deletion on bone morphometry.  $\mu$ CT analysis revealed an osteopenic phenotype in CKO mice. In femoral trabecular bone of CKO mice, we observed a 32% decrease in trabecular bone volume (BV/TV) (Fig. 1A), a 21% decrease in trabecular number (Tb.N) (Fig. 1B), a 13% decrease in trabecular thickness (Tb.Th) (Fig. 1C), and a 42% increase in trabecular spacing (Tb.Sp) (Fig. 1D) compared to CTR mice. Of note, the difference in these parameters between CTR and CHet mice is not statistically significant. There was a small but statistically significant decrease (4% and 5%, respectively) decrease in trabecular tissue mineral density (TMD) in CHet and CKO mice compared to CTR mice (Fig. 1E). The *Osx*-Cre transgene itself has no effect on femoral trabecular and cortical bone TMD (data not shown); thus, this indicated a role of FAK in regulating TMD. In femoral cortical bone of CKO mice, we observed a 24% decrease in cortical area (Fig. 1F), a 15% decrease in cortical thickness (Fig. 1G), an 11% decrease in inner cortical bone perimeter (Fig. 1H), and a 12% decrease in outer cortical bone perimeter (Fig. 1I). Similar to trabecular bone, there was a small but statistically significant decrease (3% and 2%, respectively) in cortical bone TMD in CHet and CKO mice compared to CTR mice (Fig. 1J). Of note, our previous data showed that the *Osx*-Cre transgene has minimal effect on trabecular bone volume and cortical thickness in C57BL/6 background mice.<sup>(15)</sup> In addition, CHet mice had comparable bone volume compared to CTR mice but had significantly higher bone volume compared to CKO mice. Besides femurs,  $\mu$ CT analysis was performed on calvaria. There was a decrease in bone mass in both calvarial parietal (Fig. 1K–O) and frontal (Supporting Fig. S3) bones of CKO mice compared to CTR mice. Taken together, our data showed that FAK deletion in osteoblasts leads to decreased bone mass in mice.

### Decreased bone mass in FAK-deficient mice is due to decreased osteoblastogenesis and associated with increased bone marrow adipogenesis

To determine the cellular mechanisms of FAK regulation on bone development, we performed histomorphometry on femurs of CKO and CTR mice. Consistent with  $\mu$ CT measurements, we observed decreased bone area (BA/TA) (Fig. 2A), decreased trabecular number (Tb.N) (Fig. 2B), decreased trabecular thickness (Fig. 2C), and increased trabecular spacing (Fig. 2D) in the femur of CKO mice. The osteoblast number (N.Ob/BS) (Fig. 2E) and surface (Ob.S/BS) (Fig. 2F), but not the osteoclast number (N.Oc/BS) (Fig. 2G) and surface (Oc.S/BS) (Fig. 2H), were reduced by the deletion of FAK in CKO mice. Furthermore, there were significantly increased bone marrow adipocytes in CKO mice (Fig. 2I, J). Collectively, these data suggest that compromised osteoblastogenesis associated with increased adipogenesis *in vivo* contributed to decreased bone mass in CKO mice.

### FAK deletion leads to decreased BMSC proliferation and compromised osteoblast differentiation

To further determine the mechanism responsible for the decreased osteoblastogenesis observed in CKO mice, we investigated the

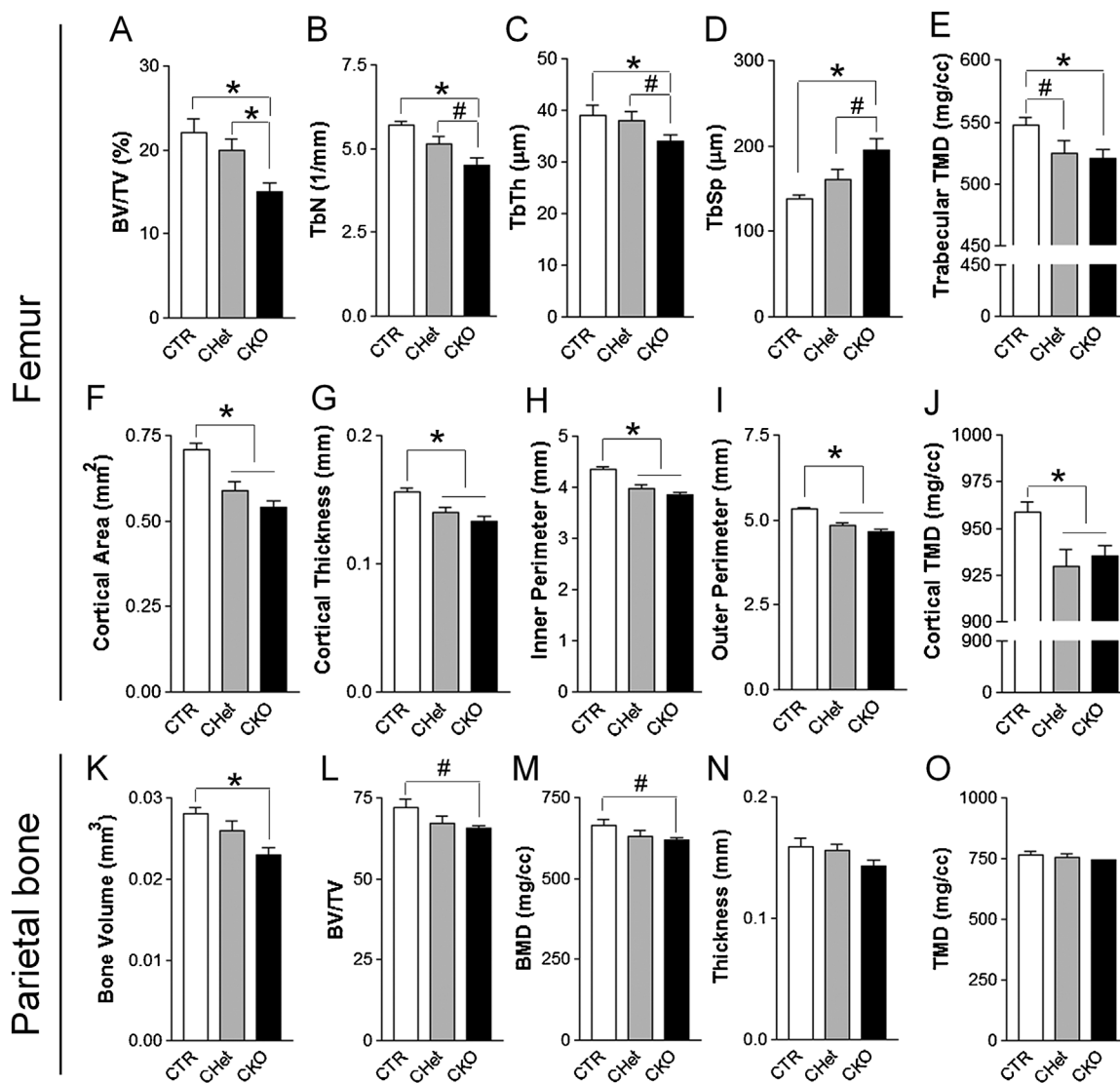


**Fig. 1.** Mice with FAK deletion exhibit reduced bone mass.  $\mu$ CT measurements were performed in femurs (A–J), and parietal bones (K–O) of 2-month-old male FAK<sup>F/F</sup> (CTR), FAK<sup>F/+</sup>;Osx-Cre (CHet), and FAK<sup>F/F</sup>;Osx-Cre (CKO) mice. (A–E) Trabecular parameters of femur: BV/TV, bone volume per tissue volume (A); Tb.N, trabecular number (B); Tb.Th, trabecular thickness (C); Tb.Sp, trabecular spacing (D); and TMD, tissue mineral density (E). (F–J) Cortical parameters of femur: cortical area (F); cortical thickness (G); inner perimeter of cortical bone (H); outer perimeter of cortical bone (I); TMD (J). (K–O) Measurement of parietal bone: bone volume (K); BV/TV (L); BMD, bone mineral density (M); parietal thickness (N); TMD (O). \* $p < 0.05$ , # $0.05 < p < 0.1$ ,  $n = 9$  to 13 per group for femoral group,  $n = 5$  to 6 per group for calvarial group. Values are presented as mean + SE.

effect of FAK deletion on osteoblast proliferation with the primary BMSC culture system. Of the cells in this culture system, 95% were Osterix<sup>+</sup> cells (data not shown). FAK was efficiently deleted in isolated BMSCs (Fig. 3A). FAK-deficient cells had compromised proliferation ability as indicated by decreased cell number and Ki67<sup>+</sup> cells (Fig. 3B–D). We then evaluated the osteogenic differentiation ability of FAK-deficient cells. FAK-deficient cells had compromised early differentiation as indicated by decreased alkaline phosphatase activity at early culture and defective terminal differentiation as indicated by poor mineralization (Fig. 4A). The expression levels of critical osteoblast differentiation transcription factors including Runx2 and Osterix were significantly decreased in CKO cultures (Fig. 4B). The expression levels of osteoblast differentiation markers, including alkaline phosphatase (Alpl),

bone sialoprotein (Bsp), Collagen, type I, alpha 1 (Colla1), and osteocalcin (Ocn) were all significantly decreased in the CKO cultures (Fig. 4B). Taken together, our data suggested that both decreased proliferation and compromised differentiation contribute to the decreased osteoblast number and bone mass in vivo.

#### FAK deletion enhances the adipogenic potential of BMSCs

Increased bone marrow adipocytes in CKO mice prompted us to assess the effect of FAK deletion on the adipogenic potential of BMSCs. Similar to osteogenic culture, the BMSCs were isolated from CTR and CKO mice and the FAK was effectively deleted (Fig. 5A). When exposed to adipogenic medium, the FAK-deficient

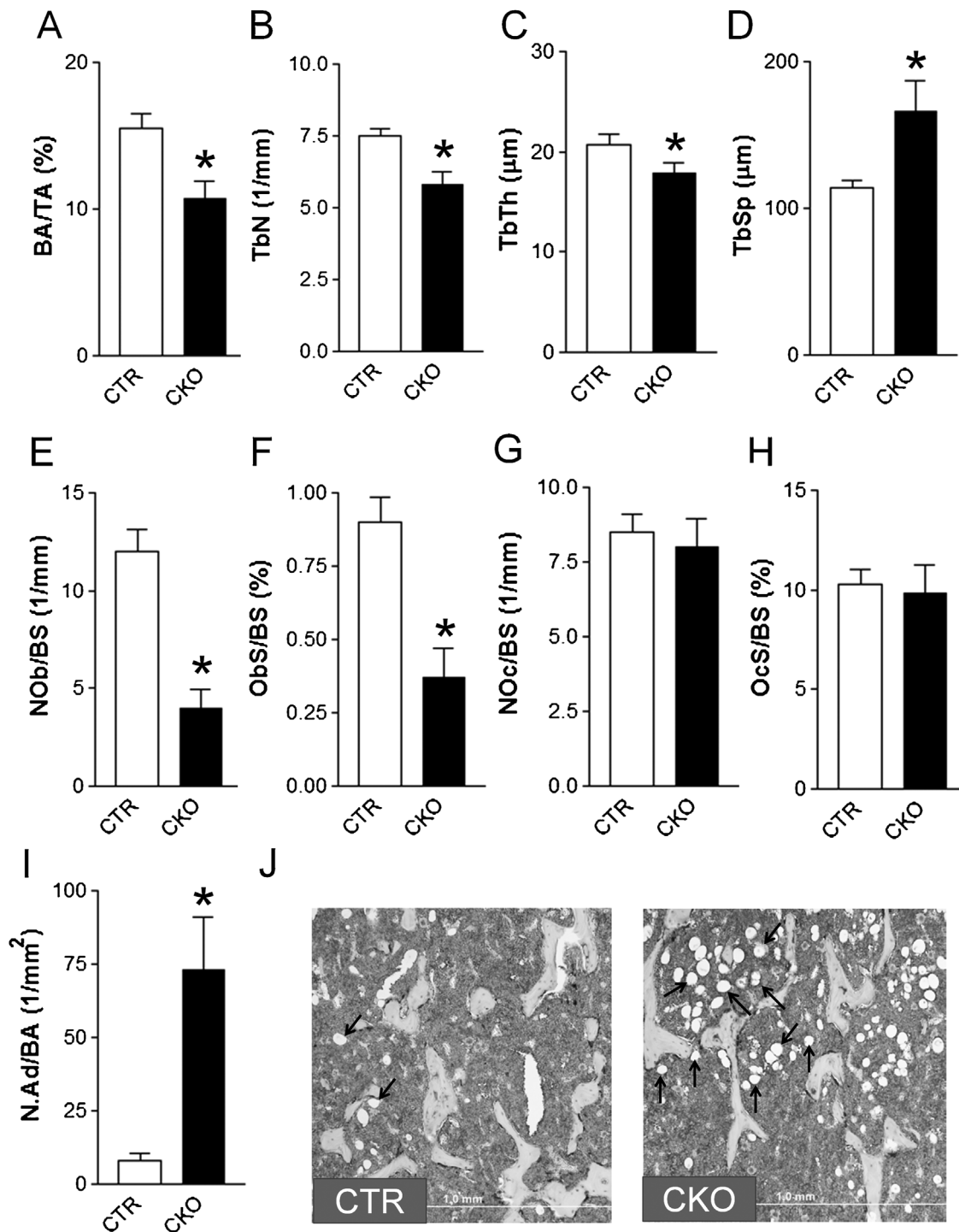


**Fig. 2.** FAK deletion in mice leads to decreased osteoblast but increased bone marrow adipocyte number. Histomorphometry analysis was performed in femur of 2-month-old FAK<sup>F/F</sup> (CTR) and FAK<sup>F/F</sup>;Osx-Cre (CKO) male mice. (A) BA/TA, bone area per tissue area. (B) Tb.N, trabecular bone number. (C) Tb.Th, trabecular thickness. (D) Tb.Sp, trabecular spacing. (E) N.Ob/BS, osteoblast number. (F) Ob.S/BS, osteoblast surface. (G) Osteoclast number. (H) Osteoclast surface. (I) N.Ad/BA, adipocyte number. (J) Histological images showing bone marrow adipocytes (indicated by arrows). \* $p < 0.05$ ,  $n = 6$  to 9. Values are presented as mean + SE.

BMSCs exhibited enhanced adipogenic differentiation, as shown by many more cells with accumulation of lipid droplets (shown by Oil Red-O staining) in CKO culture than in CTR culture (Fig. 5B, C). mRNA levels of PPAR $\gamma$ , FABP4, and Adiponectin, markers of

terminal adipogenic differentiation, were increased in FAK-deficient BMSCs (Fig. 5D). Importantly, the expression levels of these adipogenic marker genes were increased even before the adipogenic induction (day 0). Of note, PPAR $\gamma$  is not only an

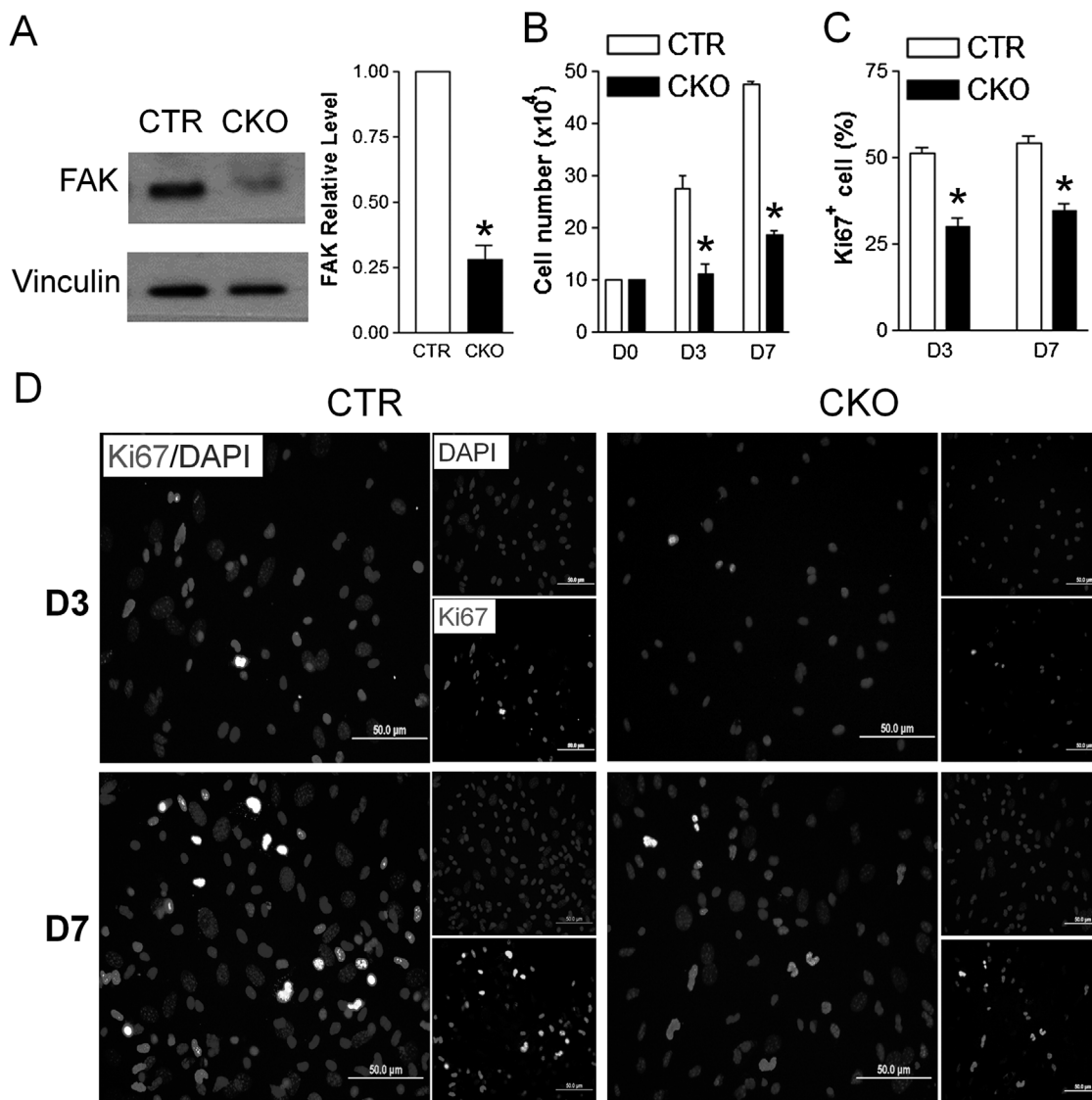


**Fig. 3.** FAK-deficient BMSCs have decreased proliferation. (A) FAK expression (left panel) and quantification (right) analyzed by Western blot in BMSCs isolated from CTR and CKO mice ( $n = 7$  per group). (B) Quantitative analysis of cell number cultured for 3 and 7 days in osteogenic medium ( $n = 4$  per group). (C) Quantification of Ki67-positive BMSCs in the cultures described in B ( $n = 3$  per group). (D) Representative fluorescent images of Ki67 (red) and Dapi (blue) staining in FAK CTR and CKO BMSCs at 3rd and 7th day, in the same cultures system as described in B. \* $p < 0.05$ . Values are presented as mean + SE.

adipogenic differentiation marker but also a vital transcription factor for adipogenic differentiation. PPAR $\gamma$  mRNA expression had a twofold increase before adipogenic induction, indicating an intrinsically enhanced adipogenic potential by FAK deletion. When cultured in adipogenic medium for 5 days, the increase of PPAR $\gamma$  mRNA expression was further augmented to fourfold in CKO culture. To address the molecular mechanisms whereby FAK deletion in BMSCs increases adipogenic ability, we next examined the expression level of other crucial adipogenic transcription factors in cultured BMSCs (Fig. 5E). Levels of mRNAs encoding CCAAT-enhancer-binding protein  $\alpha$  (C/EBP $\alpha$ ) and C/EBP $\beta$  both were increased in CKO culture. mRNA levels of zinc finger protein 423 (Zfp423), a regulator of PPAR $\gamma$  expression<sup>(22)</sup> were increased similar to PPAR $\gamma$ . Taken together, these results are consistent with the possibility that the increased adipogenesis caused by the

deletion of FAK in BMSCs was attributable to the increased expression of PPAR $\gamma$ , C/EBP $\alpha$ , C/EBP $\beta$ , and Zfp423, four essential transcription factors for adipogenesis.

#### FAK deficiency leads to decreased Wnt/ $\beta$ -catenin signaling in BMSCs

Wnt/ $\beta$ -catenin signaling regulates the adipogenic potential of BMSCs.<sup>(9,10)</sup> To determine whether altered Wnt/ $\beta$ -catenin signaling might contribute to the shift of balance between osteogenic and adipogenic potential in FAK-deficient BMSCs, we examined the  $\beta$ -catenin expression by Western blot and found reduced  $\beta$ -catenin level in FAK-deficient BMSCs throughout the osteoblast differentiation culture (Fig. 6A). Interestingly, the  $\beta$ -catenin level was positively correlated to

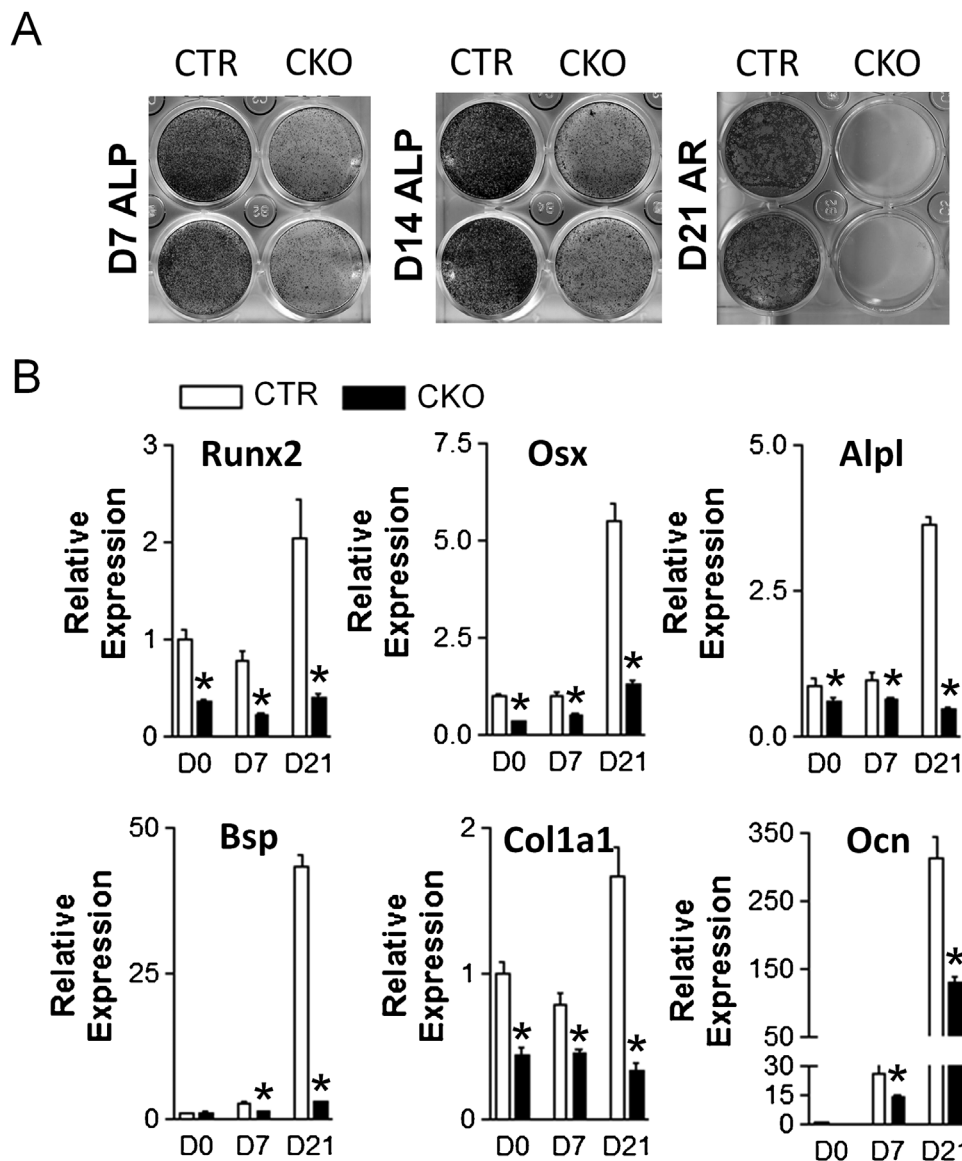


**Fig. 4.** FAK deletion compromises BMSCs osteoblast differentiation. (A) Osteoblast differentiation and mineralization from BMSCs cultured in osteogenic medium were analyzed by alkaline phosphatase (ALP) and alizarin red (AR) staining at the indicated time points. Images shown were the representatives of six independent experiments. (B) Quantitative PCR analysis of the mRNA expression of osteoblast differentiation markers, in the cultures described in A. *Osx* = osterix; *Alpl* = alkaline phosphatase; *Bsp* = bone sialoprotein protein; *Col1a1* = collagen, type 1, alpha 1; *Ocn* = osteocalcin. \* $p < 0.05$   $n = 3$ . Values are presented as mean + SE.

FAK expression level in control culture, further suggesting a role of FAK in regulating  $\beta$ -catenin level. Next, we examined the mRNA expression of Wnt target genes and found reduced expression of *Axin2*, *Cnx43*, and *Lef1* at all time points in FAK-deficient BMSCs (Fig. 6B). Therefore, deletion of FAK in BMSCs impairs Wnt signaling by downregulating its effector  $\beta$ -catenin. To further determine the underlying mechanism of attenuated Wnt/ $\beta$ -catenin signaling in FAK-deficient BMSCs, we examined the mRNA expression of some canonical Wnt ligands that are known to be expressed in *Osx*<sup>+</sup> cells.<sup>(23)</sup> We found a decrease in the expression of *Wnt1*, *Wnt3a*, and *Wnt10b* (Fig. 7A). Phosphorylation of the N terminal Ser 9 for GSK3 $\beta$  has an inhibitory effect on GSK3 function.<sup>(24)</sup> Consistent with the decrease in  $\beta$ -catenin level, the level of phosphor-GSK3 $\beta$  (S9)

was decreased in FAK-deficient BMSCs at the start of and during osteogenic differentiation (Fig. 7B), suggesting that increased degradation activity of the GSK3 complex is responsible for the increased  $\beta$ -catenin degradation and subsequent lower Wnt/ $\beta$ -catenin signaling.

FAK deficiency does not alter the proliferation or differentiation in primary calvarial osteoblast cells

To further determine the effect of FAK deletion on osteoblast proliferation and differentiation, we determined the differentiation potential of osteoblastic cells isolated from newborn calvaria, which comprise a more differentiated osteoblast population. In contrast to BMSCs, we found that both

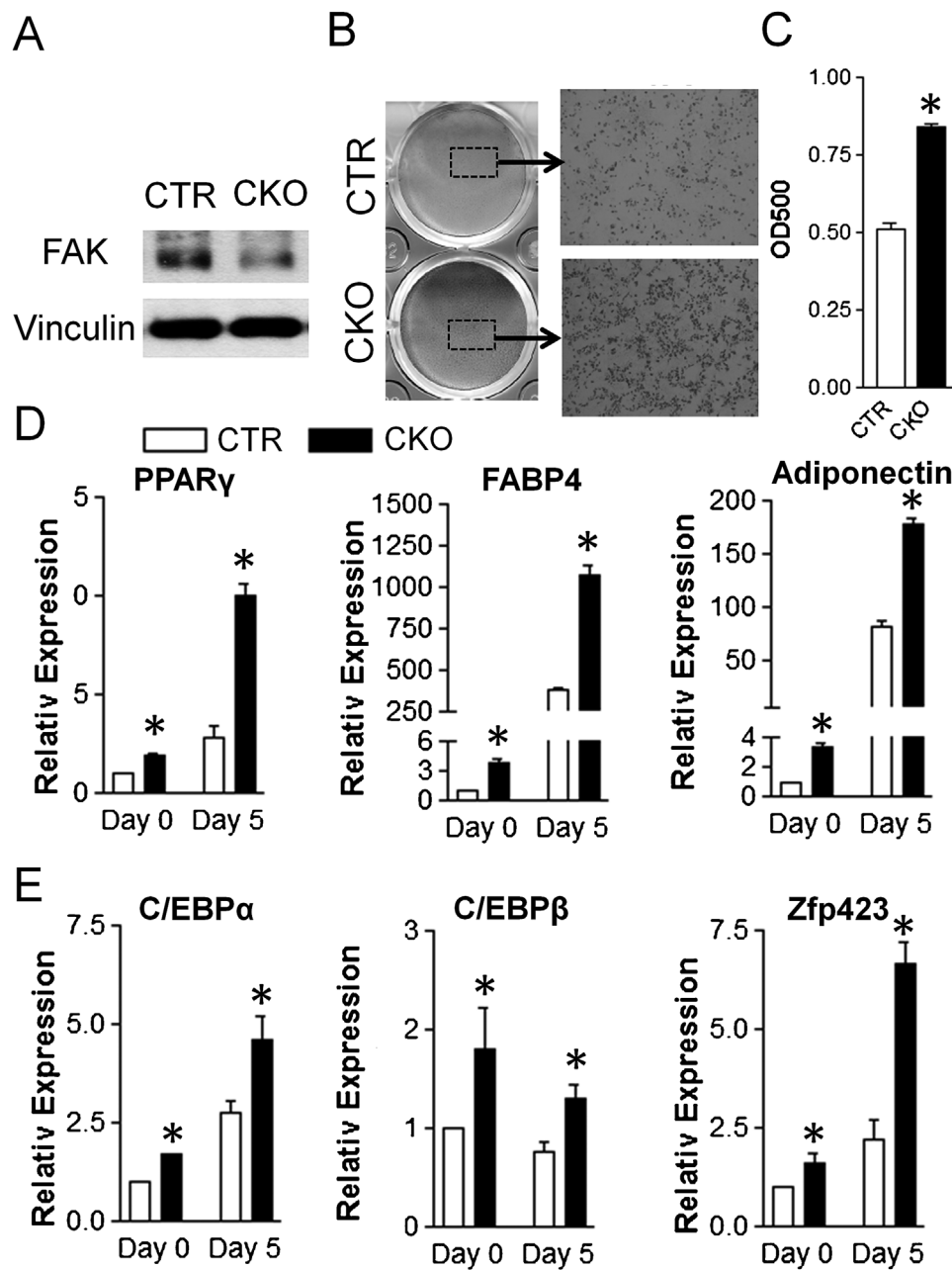


**Fig. 5.** FAK-deficient BMSCs have enhanced adipogenesis. (A) FAK was deleted in BMSCs as shown by Western blot. (B) Oil red O staining showed enhanced adipogenic differentiation of FAK-deficient BMSCs, in adipogenic medium for 5 days. (C) The quantification of Oil red O staining described in B. (D, E) Quantitative PCR analysis of the mRNA expression of adipogenic differentiation markers (D) and transcription factors that is critical for adipogenic differentiation (E), in the cultures described in B. \* $p < 0.05$   $n = 3$ . Values are presented as mean + SE.

the proliferation (Supporting Fig. S4) and differentiation (Supporting Fig. S5) were not compromised by FAK deletion in primary calvaria osteoblasts. In addition, the  $\beta$ -catenin level and mRNA expression of Wnt/ $\beta$ -catenin target genes were comparable in FAK-deficient primary calvaria osteoblasts (Supporting Fig. S6). Together, the bone marrow and calvarial culture results suggested that FAK might function at an early phase in osteoprogenitor cell proliferation and differentiation.

## Discussion

Osteoblast proliferation and differentiation are regulated by complex signaling networks and knowledge of the relationship between osteoblastogenesis and adipogenesis is important to our understanding of development and diseases affecting bone metabolism. In this work, we identified a new signaling pathway regulating the commitment of mesenchymal progenitors into the osteoblast/adipocyte lineage and the proliferation/osteogenic



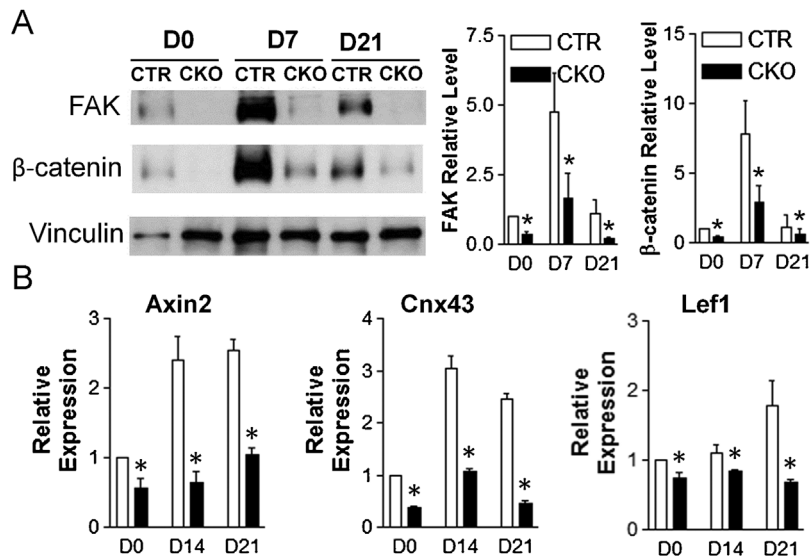


**Fig. 6.** FAK deficiency impairs Wnt/ $\beta$ -catenin signaling pathway. (A) Immunoblotting analysis (left) and quantification of FAK (middle) and  $\beta$ -catenin (right) protein level in BMSCs osteoblast differentiation cultures described in Fig. 4. (B) Quantitative PCR analysis of Wnt/ $\beta$ -catenin target gene expression during osteoblast differentiation. \* $p < 0.05$ ,  $n = 4$ . Values are presented as mean + SE.

differentiation of BMSCs. Ablation of FAK in Osterix-expressing cells leads to osteopenia and a dramatic increase in bone marrow adipogenesis associated with decreased expression of several canonical Wnt ligands, increased GSK3 activity, decreased  $\beta$ -catenin level, and decreased Wnt/ $\beta$ -catenin-mediated transcription. Because canonical Wnt signaling has been shown to promote osteoblast proliferation and differentiation and favor osteoblast over adipocyte lineage commitment,<sup>(6,8-10)</sup> we propose that the decreased Wnt/ $\beta$ -catenin signaling may at least partially account for the decreased bone mass, increased bone marrow adiposity, decreased BMSC proliferation and

osteogenic differentiation, and enhanced BMSC adipogenic differentiation (Fig. 8A, B). However, the extent that decreased Wnt/ $\beta$ -catenin signaling in FAK-deficient BMSCs is responsible for the osteopenia in CKO mice remains to be determined.

Early lineage mesenchymal cells have the ability to differentiate into various cell types including osteoblasts and adipocytes.<sup>(25)</sup> Activation of the Wnt/ $\beta$ -catenin signaling pathway promotes osteoblastogenesis and inhibits adipogenesis by regulating cell type-specific transcription factors.<sup>(26)</sup> Overexpression of Wnt1 or Wnt10b, activators of Wnt/ $\beta$ -catenin signaling, potently represses adipogenesis.<sup>(27,28)</sup> Conversely,

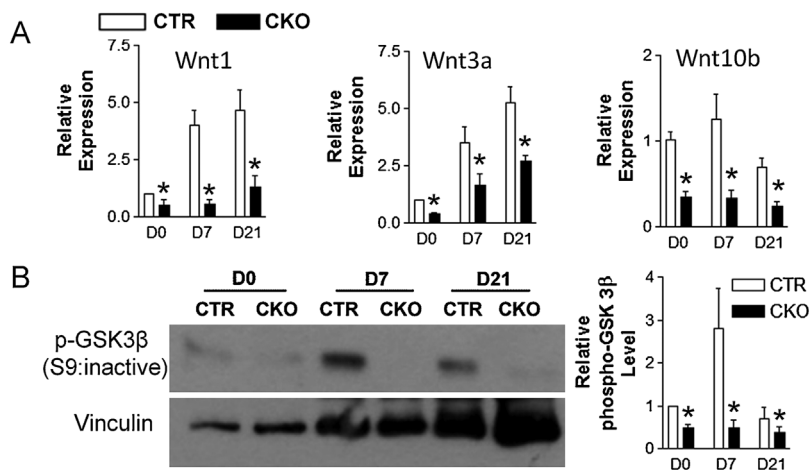


**Fig. 7.** FAK regulates Wnt/ $\beta$ -catenin signaling through Wnt ligand/GSK3 pathway. (A) mRNA levels of Wnt ligands (Wnt1, Wnt3a, and Wnt10b) by quantitative PCR in BMSCs osteoblast differentiation culture described in Fig. 4. (B) Protein levels of phosphor-GSK3 $\beta$  (p-GSK3 $\beta$ ) at S9 by Western blot (left), in the same culture shown in A. The relative level of p-GSK3 $\beta$  is shown in the right panel. \* $p < 0.05$ ,  $n = 3$ . Values are presented as mean + SE.

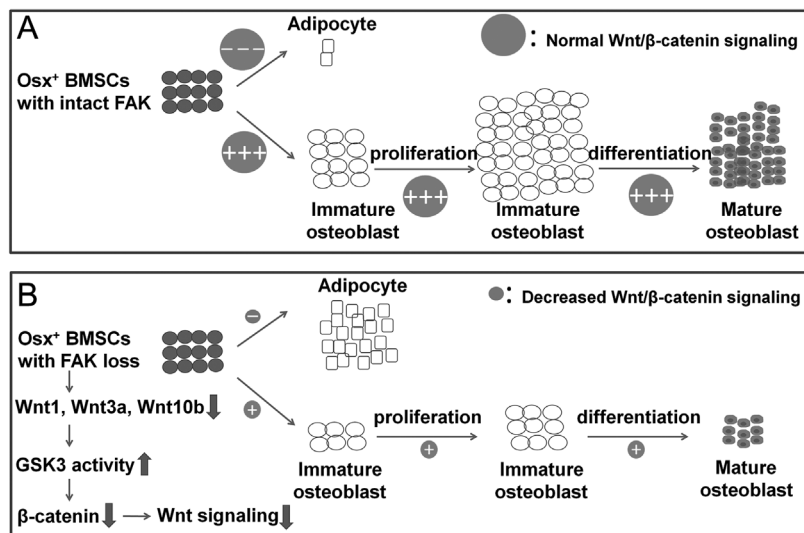


**Fig. 8.** Model of the role of FAK in regulating lineage commitment, proliferation, and osteogenic differentiation of BMSCs. (A) Wnt/β-catenin signaling pathway inhibits adipogenic differentiation of BMSCs but promotes their osteoblast lineage commitment, and positively regulates osteoblast proliferation and differentiation. (B) Ablation of FAK in early bone marrow osteoblast progenitors attenuates the expression of canonical Wnt ligands, increases GSK3 activity, decreases β-catenin level, and ultimately impairs Wnt/β-catenin-mediated transcription, which can account for the reduced BMSCs proliferation and osteogenic differentiation, but enhanced BMSCs adipogenic differentiation, and thereby contributes to the decreased bone mass and increased bone marrow adiposity. “+” indicates positive effect of Wnt/β-catenin signaling and “-” indicates inhibitory effect of Wnt/β-catenin signaling. “+++” and “---” indicate stronger promoting and inhibiting effect, respectively.

inhibition of Wnt signaling in preadipocytes stimulates differentiation.<sup>(27,29,30)</sup> Stabilization of β-catenin can promote osteoblastogenesis and inhibit adipogenesis in a bone marrow-derived cell line.<sup>(26)</sup> Overexpression of β-catenin in preadipocytes can inhibit their maturation.<sup>(27)</sup> Repression of C/EBPα and PPARγ, two critical adipogenesis transcription factors, is a primary mechanism by which Wnt signaling inhibits the differentiation of mesenchymal cells toward adipocytes. In addition, β-catenin and PPARγ can functionally interact with each other and negatively regulate each other's activity.<sup>(31,32)</sup> In FAK-deficient BMSCs, we found that Wnt/β-catenin signaling was severely compromised associated with increased expression of adipogenic transcription factors and decreased expression of osteogenic transcription factors, which could account for the aberrantly enhanced adipogenesis as well as decreased BMSC proliferation and osteogenic differentiation.

The connection between FAK and Wnt/β-catenin signaling in BMSCs is not unexpected. Hyperactivation of either Wnt/β-catenin or FAK signaling was independently shown to promote numerous types of human cancers.<sup>(33,34)</sup> In *Xenopus laevis* embryos, FAK protein knockdown anteriorizes the embryo, which resembles that of embryo knockdown for canonical Wnt signaling.<sup>(35)</sup> In addition, Wnt3a expression is FAK-dependent in developing frog neural plate.<sup>(35)</sup> In MCF-7 cells, a human breast cancer cell line, FAK protein depletion reduces Wnt3 and Wnt3a expression.<sup>(35)</sup> The similar regulation of Wnt ligand between frog and human cell line suggests that FAK regulation on Wnt signaling pathway could be highly conserved among vertebrates. Here we present the evidence showing the similar FAK/Wnt regulation axis in mouse.

A previous report showed that loss of FAK in osteoblasts leads to delayed bone regeneration and defective bone matrix deposition in a fracture healing model as well as compromised

osteoblast differentiation in clonally established cell lines.<sup>(13)</sup> Here we report that FAK plays important role in bone development and bone marrow osteoblast differentiation. Of note, different transgenic Cre mouse models were used in these two studies. In the aforementioned report, Cre recombinase is driven by 2.3 kb of the collagen type I (α)I promoter.<sup>(13)</sup> It is known that this promoter is active in mature osteoblasts.<sup>(36,37)</sup> In our current research, Cre recombinase is driven by the Osterix promoter, which is active in earlier osteoblast lineage cells.<sup>(8)</sup> Most recently, lineage-tracing experiments showed that Osterix-expressing cells labeled during early embryo development can give rise to both osteoblasts and adipocytes *in vivo*.<sup>(38)</sup> In contrast to the defective proliferation, differentiation, and Wnt/β-catenin signaling pathway in FAK-deficient BMSCs, there was no abnormality in the *in vitro* culture of FAK-deficient primary calvarial osteoblasts. It is not uncommon to observe the different effects of gene deletion on osteogenic differentiation between bone marrow osteoblasts and calvarial osteoblasts. The deletion of Pyk2, another FAK subfamily member, leads to altered bone marrow osteoblast differentiation but not to more mature calvarial osteoblasts.<sup>(39)</sup> This disparity of the effects of FAK deletion in BMSCs versus calvarial osteoblasts may be due to several possible reasons. First, FAK deletion has cell origin-specific (bone marrow versus calvaria) effects on osteoblasts. However, there was also decreased calvarial bone mass in CKO mice, which argues against this possibility. Second, because BMSCs are a mixed cell population, there might be much fewer osteoblasts in BMSCs from CKO mice. In our BMSC culture system, we found that 95% of attached cells are Osterix<sup>+</sup> prior to the osteogenic differentiation experiment (data not shown). Thus there were enriched Osterix<sup>+</sup> cells in BMSC cultures comparable to that in calvarial cultures. Third, FAK deletion has a differentiation stage-specific (progenitor versus more mature)

effect on osteoblast function. Even though calvarial osteoblasts are also originally from Osterix-expressing osteoprogenitor cells *in vivo*, the isolated calvarial cells represent a more differentiated population.

Conditional  $\beta$ -catenin deletion in mature osteoblastic lineage cells leads to an osteopenia phenotype through the increase in osteoblastogenesis as a result of increased expression of osteoprotegerin (OPG), a major inhibitor of osteoclast differentiation.<sup>(40,41)</sup> In FAK CKO mice with the *Osx*-Cre driver, our data showed that osteoclast number was not affected. This may explain the phenotypic difference between the  $\beta$ -catenin CKO model and the FAK CKO model when later osteoblastic lineage cells are targeted. However, it is unknown whether there is alteration in osteoclastogenesis (or osteoblastogenesis) in FAK CKO mice with the *Col2.3*-Cre model.<sup>(13)</sup>

Our findings suggest that in Osterix-expressing cells, FAK promotes Wnt signaling, thereby increasing the number of matrix-synthesizing osteoblasts by promoting their proliferation and decreasing their adipocyte lineage commitment, and enhancing their osteogenic differentiation, and thus ultimately increases bone mass. It has been reported that Osterix-Cre targets multiple cell types besides the osteoblast lineage in postnatal mice.<sup>(42)</sup> Thus, the bone phenotype is potentially contributed by other non-osteoblast lineage cells. Noteworthy, the skeletal phenotype of FAK CKO mice is much milder than that of  $\beta$ -catenin CKO mice using the same Cre driver,<sup>(8)</sup> which may reflect the fact that  $\beta$ -catenin was decreased but not ablated in FAK CKO mice. The finding that FAK signaling plays a critical role in determining bone and marrow fat mass suggests the potential adverse skeletal consequence of using FAK signaling inhibitors in treating various cancer patients.<sup>(14)</sup> Because FAK inhibitor administration inhibits FAK activity systemically, it would be important to understand how FAK inhibition could affect the function of earlier mesenchymal lineage cells, which could not be addressed by the Osterix-Cre model and warrants the use of other mouse models.

## Disclosures

All authors state that they have no conflicts of interest.

## Acknowledgments

This work was supported by grants from the NIH (R01AR062030 to FL, R01CA163493 to JG, and DE016530 to PHK) and the National Natural Science Foundation of China (award number 31201039 to CS). The content is solely the responsibility of the authors and does not necessarily represent the official views of the NIH. We thank Ms. Jaclynn Kreider and Basma Khoury for  $\mu$ CT scanning and reconstruction.

Authors' roles: Study design: CS, HY, LW, JG, and FL. Data acquisition: CS, HY, LW, XW, PHK, and FL. Data analysis and interpretation: CS, HY, LW, XW, PHK, JG, and FL. Drafting manuscript: CS and FL. Approving final version of manuscript: CS, HY, LW, XW, PHK, JG, and FL. FL takes responsibility for the integrity of the data analysis.

## References

1. Justesen J, Stenderup K, Ebbesen EN, Mosekilde L, Steiniche T, Kassem M. Adipocyte tissue volume in bone marrow is increased with aging and in patients with osteoporosis. *Biogerontology*. 2001;2(3):165–71.
2. Minaire P, Neunier P, Edouard C, Bernard J, Courpron P, Bourret J. Quantitative histological data on disuse osteoporosis: comparison with biological data. *Calcif Tissue Res*. 1974;17(1):57–73.
3. Wronski TJ, Morey-Holton E, Jee WS. Skeletal alterations in rats during space flight. *Adv Space Res*. 1981;1(14):135–40.
4. Nuttall ME, Gimble JM. Is there a therapeutic opportunity to either prevent or treat osteopenic disorders by inhibiting marrow adipogenesis? *Bone*. 2000;27(2):177–84.
5. Krebsbach PH, Kuznetsov SA, Bianco P, Robey PG. Bone marrow stromal cells: characterization and clinical application. *Crit Rev Oral Biol Med*. 1999;10(2):165–81.
6. Prestwich TC, Macdougald OA. Wnt/ $\beta$ -catenin signaling in adipogenesis and metabolism. *Curr Opin Cell Biol*. 2007;19(6):612–7.
7. Liu F, Kohlmeier S, Wang CY. Wnt signaling and skeletal development. *Cell Signal*. 2008;20(6):999–1009.
8. Rodda SJ, McMahon AP. Distinct roles for Hedgehog and canonical Wnt signaling in specification, differentiation and maintenance of osteoblast progenitors. *Development*. 2006;133(16):3231–44.
9. Song L, Liu M, Ono N, Bringham FR, Kronenberg HM, Guo J. Loss of wnt/ $\beta$ -catenin signaling causes cell fate shift of preosteoblasts from osteoblasts to adipocytes. *J Bone Miner Res*. 2012;27(11):2344–58.
10. Chen J, Long F.  $\beta$ -catenin promotes bone formation and suppresses bone resorption in postnatal growing mice. *J Bone Miner Res*. 2013;28(5):1160–9.
11. Luo M, Guan JL. Focal adhesion kinase: a prominent determinant in breast cancer initiation, progression and metastasis. *Cancer Lett*. 2010;289(2):127–39.
12. Schaller MD. Cellular functions of FAK kinases: insight into molecular mechanisms and novel functions. *J Cell Sci*. 2010;123(Pt 7):1007–13.
13. Kim JB, Leucht P, Luppen CA, et al. Reconciling the roles of FAK in osteoblast differentiation, osteoclast remodeling, and bone regeneration. *Bone*. 2007;41(1):39–51.
14. Sulzmaier FJ, Jean C, Schlaepfer DD. FAK in cancer: mechanistic findings and clinical applications. *Nat Rev Cancer*. 2014;14(9):598–610.
15. Liu F, Fang F, Yuan H, et al. Suppression of autophagy by FIP200 deletion leads to osteopenia in mice through the inhibition of osteoblast terminal differentiation. *J Bone Miner Res*. 2013;28(11):2414–30.
16. Shen TL, Park AY, Alcaraz A, et al. Conditional knockout of focal adhesion kinase in endothelial cells reveals its role in angiogenesis and vascular development in late embryogenesis. *J Cell Biol*. 2005;169(6):941–52.
17. Fang F, Sun S, Wang L, et al. Neural crest-specific TSC1 deletion in mice leads to sclerotic craniofacial bone lesion. *J Bone Miner Res*. 2015;30(7):1195–205.
18. Wang J, Xi L, Hunt JL, et al. Expression pattern of chemokine receptor 6 (CCR6) and CCR7 in squamous cell carcinoma of the head and neck identifies a novel metastatic phenotype. *Cancer Res*. 2004;64(5):1861–6.
19. Liu J, Nam HK, Campbell C, Gasque KC, Millan JL, Hatch NE. Tissue-nonspecific alkaline phosphatase deficiency causes abnormal craniofacial bone development in the *Alpl*( $-/-$ ) mouse model of infantile hypophosphatasia. *Bone*. 2014;67:81–94.
20. Chandhoke TK, Huang YF, Liu F, et al. Osteopenia in transgenic mice with osteoblast-targeted expression of the inducible cAMP early repressor. *Bone*. 2008;43(1):101–9.
21. Dempster DW, Compston JE, Drezner MK, et al. Standardized nomenclature, symbols, and units for bone histomorphometry: a 2012 update of the report of the ASBMR Histomorphometry Nomenclature Committee. *J Bone Miner Res*. 2013;28(1):2–17.
22. Gupta RK, Arany Z, Seale P, et al. Transcriptional control of preadipocyte determination by Zfp423. *Nature*. 2010;464(7288):619–23.
23. Tan SH, Senarath-Yapa K, Chung MT, Longaker MT, Wu JY, Nusse R. Wnts produced by Osterix-expressing osteolineage cells regulate their proliferation and differentiation. *Proc Natl Acad Sci U S A*. 2014;111(49):E5262–71.

24. Rayasam GV, Tulasi VK, Sodhi R, Davis JA, Ray A. Glycogen synthase kinase 3: more than a namesake. *Br J Pharmacol.* 2009;156(6):885–98.
25. Krishnan V, Bryant HU, Macdougald OA. Regulation of bone mass by Wnt signaling. *J Clin Invest.* 2006;116(5):1202–9.
26. Bennett CN, Longo KA, Wright WS, et al. Regulation of osteoblastogenesis and bone mass by Wnt10b. *Proc Natl Acad Sci U S A.* 2005;102(9):3324–9.
27. Ross SE, Hemati N, Longo KA, et al. Inhibition of adipogenesis by Wnt signaling. *Science.* 2000;289(5481):950–3.
28. Moldes M, Zuo Y, Morrison RF, et al. Peroxisome-proliferator-activated receptor gamma suppresses Wnt/beta-catenin signalling during adipogenesis. *Biochem J.* 2003;376(Pt 3):607–13.
29. Bennett CN, Ross SE, Longo KA, et al. Regulation of Wnt signaling during adipogenesis. *J Biol Chem.* 2002;277(34):30998–1004.
30. Li FQ, Singh AM, Mofunanya A, et al. Chibby promotes adipocyte differentiation through inhibition of beta-catenin signaling. *Mol Cell Biol.* 2007;27(12):4347–54.
31. Liu J, Farmer SR. Regulating the balance between peroxisome proliferator-activated receptor gamma and beta-catenin signaling during adipogenesis. A glycogen synthase kinase 3beta phosphorylation-defective mutant of beta-catenin inhibits expression of a subset of adipogenic genes. *J Biol Chem.* 2004;279(43):45020–7.
32. Liu J, Wang H, Zuo Y, Farmer SR. Functional interaction between peroxisome proliferator-activated receptor gamma and beta-catenin. *Mol Cell Biol.* 2006;26(15):5827–37.
33. Golubovskaya VM. Targeting FAK in human cancer: from finding to first clinical trials. *Front Biosci (Landmark Ed).* 2014;19:687–706.
34. Fonar Y, Frank D. FAK and WNT signaling: the meeting of two pathways in cancer and development. *Anticancer Agents Med Chem.* 2011;11(7):600–6.
35. Fonar Y, Gutkovich YE, Root H, et al. Focal adhesion kinase protein regulates Wnt3a gene expression to control cell fate specification in the developing neural plate. *Mol Biol Cell.* 2011;22(13):2409–21.
36. Dacquin R, Starbuck M, Schinke T, Karsenty G. Mouse alpha1(I)-collagen promoter is the best known promoter to drive efficient Cre recombinase expression in osteoblast. *Dev Dyn.* 2002;224(2):245–51.
37. Liu F, Woitge HW, Braut A, et al. Expression and activity of osteoblast-targeted Cre recombinase transgenes in murine skeletal tissues. *Int J Dev Biol.* 2004;48(7):645–53.
38. Liu Y, Strecker S, Wang L, et al. Osterix-cre labeled progenitor cells contribute to the formation and maintenance of the bone marrow stroma. *PLoS One.* 2013;8(8):e71318.
39. Buckbinder L, Crawford DT, Qi H, et al. Proline-rich tyrosine kinase 2 regulates osteoprogenitor cells and bone formation, and offers an anabolic treatment approach for osteoporosis. *Proc Natl Acad Sci U S A.* 2007;104(25):10619–24.
40. Glass DA 2nd, Bialek P, Ahn JD, et al. Canonical Wnt signaling in differentiated osteoblasts controls osteoclast differentiation. *Dev Cell.* 2005;8(5):751–64.
41. Kramer I, Halleux C, Keller H, et al. Osteocyte Wnt/beta-catenin signaling is required for normal bone homeostasis. *Mol Cell Biol.* 2010;30(12):3071–85.
42. Chen J, Shi Y, Regan J, Karupiah K, Ornitz DM, Long F. Osx-Cre targets multiple cell types besides osteoblast lineage in postnatal mice. *PLoS One.* 2014;9(1):e85161.